Stretching Isotactic Polypropylene: From "cross-β" to Crosshatches, from γ Form to α Form

Finizia Auriemma* and Claudio De Rosa

Dipartimento di Chimica, Università di Napoli "Federico II", Complesso Monte Sant' Angelo, via Cintia, 80126 Napoli, Italy

Received April 24, 2006; Revised Manuscript Received July 18, 2006

ABSTRACT: A method for the detailed analysis of the possible crystalline structures and preferred orientations of crystals that develop during stretching metallocene-made isotactic polypropylene (iPP) samples is presented. The analysis is illustrated in the case of various iPP samples characterized by a different distribution of stereodefects along the chain, generated by different catalysts. The method is based on the calculation of schematic X-ray fiber diffraction patterns of model structures and the comparison between calculated and experimental diffraction patterns recorded during stretching. The analyzed samples, initially crystallized in the γ form or in disordered modifications intermediate between the α and γ forms, undergo structural and morphological transformations during stretching. At low deformations, crystals of the γ form are oriented with chain axes directed nearly perpendicular to the stretching direction. The γ form gradually transforms into the α form, with chain axes parallel to the stretching direction, with increasing deformation. At high deformations, when the sample is almost totally crystallized in the α form, the crosshatched morphology, characterized by the presence of daughter lamellae epitaxially grown on mother lamellae, develops. The origin of the nonstandard orientation of crystals of the γ form with chain axes perpendicular to the fiber axis (perpendicular chain axis orientation or "cross-β") is investigated. This kind of preferred crystal orientation involves lamellae of the γ form frozen in strained regions of the polymer matrix. Its development may be ascribed to the peculiar architecture of the γ form, consisting in a nearly perpendicular arrangement of the chain axes in the unit cell, and to the elongated shape of the γ lamellae in the direction normal, rather than parallel, to the chain axes. At low draw ratios, the chain axes, which emerge at the crystal boundaries according to two mutually perpendicular directions, act as anchors for the crystals of the γ form in the perpendicular chain axis orientation. At high draw ratios, these crystals transform into the α form and assume the orientation with chain axes parallel to the stretching direction as in the standard fiber morphology. The relationships between structure and morphology on one hand and mechanical properties of the analyzed iPP samples on the other hand are also discussed.

Introduction

The structural and morphological transformations induced by uniaxial drawing of isotactic polypropylene (iPP) have been widely studied under a large number of processing conditions.[1−8] The crystalline forms and the morphology obtained during processing depend on the processing conditions[1,7] and the microstructure of the chains.[9−16]

The studies performed so far have been mainly focused on Ziegler−Natta (ZN) iPP samples.[1−8] In the case of metallocene-made iPP, instead, there are only few studies concerning the polymorphism and the mechanical properties in oriented fibers.[9−16] The crystallization properties of metallocene-made iPP have been mainly studied in the case of unoriented samples crystallized from the melt.[15,17−21] These studies have clearly demonstrated that metallocene-made iPP samples present crystallization behavior and physical properties completely different from those of ZN iPP due to the different microstructures of chains produced with metallocene and ZN catalysts.[22] In fact, the polymorphic behavior of iPP is related to the type and distribution along the chains of defects of stereoregularity and regioregularity, generated by the catalytic systems.[9−11,15−26] Since the fine-tuning of iPP microstructure is nowadays possible by choosing "ad hoc" the catalytic system, iPP samples presenting desired physical properties may be easily obtained.[15,27] It is, therefore, expected that metallocene-made iPPs display different structural and morphological transformations during deformation and processing depending on the microstructure and different from those shown by ZN iPP.

The mechanical properties of metallocene-made iPP samples of different stereoregularity containing only variable amounts of isolated *rr* triad stereodefects have been investigated in recent papers.[14−16] Depending on the concentration of *rr* defects, stiff-plastic (with low content of *rr* defects, up to 3−4%, and melting temperatures in the range 160−130 °C), flexible-plastic (with 4−6% of *rr* defects and melting temperatures around 115−120 °C), and elastic (with 7−11% of *rr* defects and melting temperature in the range 80−110 °C) polypropylene materials have been obtained. The high flexibility of stereoregular samples is related to the polymorphic transformations of α and γ forms into the mesomorphic form by stretching, whereas the elastic behavior of less crystalline and stereoregular samples is associated with a reversible polymorphic transition between the mesomorphic form and the α form of iPP, occurring during stretching and relaxation.[15,16]

Furthermore, it has been shown that using particular metallocene catalysts based on C_2-symmetric zirconocene, poorly isotactic, nearly amorphous polypropylenes (*iam*-PP), with a concentration of *mmmm* pentad of 35% and a random distribution of defects, showing elastomeric properties may be produced.[28] These materials crystallize in disordered modifications intermediate between the α and γ forms, similar to the γ form, that gradually transform by stretching at high deformations into structures more similar to the α form.[13,14]

* Corresponding author. E-mail: Finizia.Auriemma@unina.it. Telephone: ++39 081 674341. Fax: ++39 081 674090.

10.1021/ma0609127 CCC: $33.50
Published on Web 10/03/2006

Table 1. Polymerization Temperatures (T_{pol}), Concentrations of Pentad *mmmm* and Diad *m*, Molecular Masses (M_w), Polydispersity Indices (M_w/M_n), and Melting Temperatures (T_m) of iPP Samples R, W, and of the Fractions of the Sample W Soluble in Boiling Diethyl Ether (W(ES)) and Heptane (W(HS))[a]

samples	T_{pol} (°C)	[*mmmm*] (%)	[*m*] (%)	[*mm*] (%)	[*mr*] (%)	[*rr*] (%)	M_w	M_w/M_n	T_m[d] (°C)
R[b]	60	83.4	93.1	89.7	6.9	3.4	66000	~2	137
W[c]	50	34	73	-	-	-	201000	2.3	65−155[e]
W(HS)[c]	-	44	79	-	-	-	220000	2.3	70
W(ES)[c]	-	21	67	-	-	-	147000	2.1	-

[a] The distribution of steric triads of the sample R is also reported. [b] Prepared with *rac*-isopropylidene[bis(3-trimethylsilyl)(indenyl)]zirconium/MAO catalytic system as described in ref 35. Concentration of steric diads, triads, and pentads determined by ^{13}C NMR analysis.[35] Average molecular weight determined by GPC analysis.[35] [c] Prepared with bis[2-(3,5-di-*tert*-butylphenyl)indenyl]hafnium dichloride/MAO catalytic system and fractionated as described in ref 9. Concentration of steric diads and pentads determined by ^{13}C NMR analysis.[9] Average molecular weight and polydispersity index determined by GPC analysis.[9] [d] Determined by DSC at heating rate of 10 °C/min, flowing N_2 atmosphere.[19] [e] The DSC scan of sample W presents two melting peaks at 65 and 155 °C.[9,20]

The frequent presence of the γ form in metallocene-made iPP samples, even in stretched fibers, complicates noticeably the morphologies and textures that develop during uniaxial drawing. The complex textures make the interpretation of diffraction data a not straightforward task, owing to the similarity of diffraction patterns of the α and γ forms[29,30] and the peculiar morphologies that α and γ forms may develop.[17,31] Moreover, the presence of structural disorder, the low degree of crystallinity, the small dimensions of crystals, the presence of the amorphous phase, and/or the simultaneous presence of different crystalline forms in stretched samples make the analysis of the diffraction data rather complicated. In fact, these factors create a large amount of background intensity and the characteristic diffraction peaks of the crystalline forms appear broad, of low intensity, and superimposed.

A deep comprehension of the kind of preferential orientation that iPP crystals assume in stretched samples depending on the chain microstructure is of great importance to exploit the metallocene catalyst technology that allows the fine-tuning of the chain microstructure and may afford obtaining products with enhanced and unprecedented mechanical properties.[27]

This paper presents a deep analysis of the structural and morphological transformations that may occur during stretching in melt-crystallized iPP samples initially crystallized in the γ form or in disordered modifications intermediate between the α and γ forms. The study is illustrated in the case of iPP samples prepared using different metallocene catalysts and characterized by a different microstructure, chosen as representative examples. This analysis may be of more general interest, owing to the possibility of nucleating different crystalline polymorphs and of inducing preferential orientation of crystals by epitaxy.[32−34]

Experimental Procedure and Calculation Method of X-ray Diffraction Patterns

Three different iPP samples, prepared with two different kinds of metallocene catalysts, have been studied. Sample R was synthesized at 60 °C using the single-center metallocene catalyst composed of *rac*-isopropylidene[bis(3-trimethylsilyl)(indenyl)]zirconium dichloride, activated with methylaluminoxane (MAO), as described in ref 35. This catalytic system is highly regiospecific and produces relatively high molecular weight iPP samples (the polydispersity index of the molecular masses is around 2) with a random distribution of defects of stereoregularity, mainly represented by isolated *rr* triads.[35] The molecular mass, the melting temperature, the concentrations of pentad *mmmm* and diad *m*, and the distribution of steric triads of the sample R are reported in Table 1.

The elastomeric sample W was prepared using the unbridged metallocene catalyst bis[2-(3,5-di-*tert*-butylphenyl)indenyl]hafnium dichloride, activated with MAO in liquid propylene, as described in ref 9. These types of unbridged complexes are able to interconvert between chiral and achiral torsional isomers on the time scale of the polymerization reaction, producing a reactor blend of polypropylene, which can be separated in fractions of different tacticities and melting temperatures. The different fractions are characterized by chains with an isotactic and atactic stereoblock structure.[9−11,20,23−25] The unfractioned sample presents a low degree of stereoregularity ([*mmmm*] = 34%) and molecular weight M_w = 201 000.[9] The sample has been fractioned with boiling ethyl ether and heptane, to yield an ether-soluble fraction (W(ES)) with low stereoregularity, a fraction soluble in heptane and insoluble in ether (W(HS)) with intermediate stereoregularity, and a heptane-insoluble fraction (W(HI)) with high stereoregularity. The relative amount of the three fractions are 48, 42, and 10%, respectively.[9] We have analyzed the heptane-soluble (W(HS)) and the ether-soluble (W(ES)) fractions. The main properties of these fractions are summarized in Table 1. The fraction W(HS) melts at 70 °C, whereas the fraction W(ES) is amorphous in the unstretched state but crystallizes by stretching.

Unoriented films used for the structural analysis have been obtained by compression molding. The powder samples have been heated at 200 °C between perfectly flat brass plates under a press at very low pressure, kept at 200 °C for 10 min, and slowly cooled to room temperature.

Oriented fibers have been obtained by stretching compression-molded films up to a given strain ϵ, defined as $\epsilon = 100\ (l - l_0)/l_0$ with l_0 and l the initial and final lengths of the sample, respectively. In the case of elastomeric samples (W(ES) and W(HS)), stress-relaxed fibers have been prepared by stretching the compression molded films up to a given strain ϵ, keeping the fibers under tension for 2 h at room temperature, then removing the tension. These stress-relaxed fibers have been defined fibers W(ES)-ϵ and W(HS)-ϵ. The residual deformation after removing the tension (tension set) is in all cases small regardless of the maximum strain achieved by stretching.[10]

X-ray diffraction patterns have been obtained with Ni-filtered Cu Kα radiation. The powder profiles were obtained with an automatic Philips diffractometer, whereas the fiber diffraction patterns were recorded on a BAS-MS imaging plate (FUJIFILM) using a cylindrical camera and processed with a digital imaging reader (FUJIBAS 1800).

The method used for the calculation of the X-ray intensity distribution of iPP in the α and γ forms or in intermediate modifications containing various amounts of α/γ disorder has been developed in ref 13 for the modeling of fiber diffraction patterns and in ref 19 for the modeling of powder diffraction profiles. The X-ray modeling of fibers with crystals in cross-β orientation (perpendicular chain axis orientation) may be easily included in the treatment of ref 13 because it corresponds to model domains of α or γ form, or of disordered modifications intermediate between the α and γ forms, oriented with the axes b_α of the α form, and c_γ of the γ form, parallel to the fiber axis.

Possible Kinds of Structural Disorder and Preferred Orientation of α and γ Forms

The crystal structures of α and γ forms of iPP are very similar. The limit-ordered structural models proposed for the α

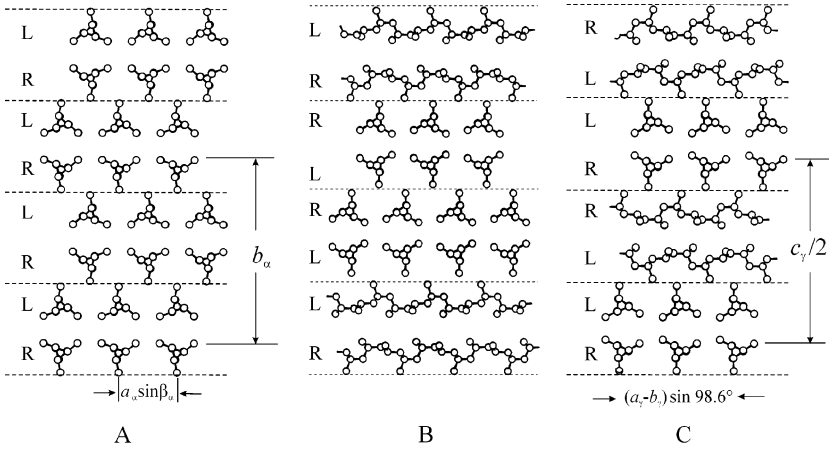

Figure 1. Limit ordered models of packing proposed for α (A) and γ (C) forms of iPP and model of the α/γ disordered modifications intermediate between α and γ forms (B). The dashed horizontal lines delimit bilayers of chains. Subscripts α and γ identify unit cell parameters referred to the monoclinic[30] and orthorhombic[29] unit cells of the α and γ forms, respectively. In the disordered model (B), consecutive bilayers of chains are stacked along b_α (c_γ) with the chain axes either parallel, as in the α form, or nearly perpendicular, as in the γ form.[13,19] Symbols R and L indicate rows of all right- and left-handed helical chains, respectively.

and γ forms are shown in Figure 1. Both the α and γ forms are characterized by chains in the 3/1 helical conformation (chain periodicity $c = 6.5$ Å), organized to form bilayers. However, α form is characterized by a regular stacking of bilayers along the b_α-axis direction with chain axes all parallel[30] (Figure 1A), whereas the γ form is characterized by a regular packing along the c_γ-axis direction of bilayers of chains with axes oriented alternatively along two nearly perpendicular directions[29] (Figure 1C). The angle between the axes of chains belonging to consecutive bilayers is 98.6° (or equivalently 81°), close to the angle β_α of the monoclinic unit cell of the α form.

As a consequence of the structural similarity, the X-ray diffraction patterns of α and γ forms of iPP are very similar. The calculated powder diffraction profiles of crystals of pure α and γ forms are shown in Figure 2. The most intense diffraction peaks of the α form occur at $2\theta = 14.2$, 17.1, 18.6, 21.1, and 21.8° ($d = 6.25$, 5.18, 4.76, 4.18, and 4.06 Å, respectively) and correspond to $(110)_\alpha$, $(040)_\alpha$, $(130)_\alpha$, $(111)_\alpha$, and $(\bar{1}31)_\alpha + (041)_\alpha$ reflections, respectively (Figure 2a).[30] The most characteristic diffraction peaks of the γ form occur at $2\theta = 13.8$, 16.7, 20.1, 21.2, and 21.9°, ($d = 6.40$, 5.30, 4.42, 4.19, and 4.06 Å, respectively) and correspond to $(111)_\gamma$, $(008)_\gamma$, $(117)_\gamma$, $(202)_\gamma$, and $(026)_\gamma$ reflections, respectively (Figure 2c).[29] The only remarkable difference in the diffraction patterns of α and γ forms is in the position of the third strong peak which occurs at $2\theta = 18.6°$ ($(040)_\alpha$ reflection) for the α form, and at $2\theta = 20.1°$ ($(008)_\gamma$ reflection) for the γ form.

Crystals of γ form obtained in metallocene-made iPP samples generally present structural disorder, characterized by defects in the regular stacking of bilayers of chains.[13−15,19] An example of a disordered modification is shown in Figure 1B. In this structure, consecutive bilayers of chains may face each other with the chain axes either parallel (like in the α form, Figure 1A) or nearly perpendicular (like in the γ form, Figure 1C). A continuum of disordered modifications intermediate between the α and γ forms of iPP may be obtained, depending on the microstructure and the thermal and mechanical history of the sample.[13−16,19,20]

As shown in refs 13 and 19, the presence of structural disorder in the crystalline domains of the kind shown in Figure 1B (α/γ disorder) induces fluctuations in the relative intensities of the Bragg peaks and introduces some diffuse scattering in the X-ray diffraction patterns. The X-ray powder diffraction profile calculated for a model of disordered modification intermediate between the α and γ forms, characterized by a statistical succession of bilayers with chains parallel or perpendicular, including an equal fraction of consecutive bilayers of chains faced as in the α (f_α) and γ (f_γ) forms ($f_\alpha = f_\gamma = 0.5$), is shown in Figure 2b. The diffuse scattering concentrates in very narrow regions of the diffraction patterns, i.e., at $2\theta \approx 14°$, around the $(110)_\alpha$ and $(111)_\gamma$ reflections of the α and γ forms, respectively, and in the 2θ range 18−20°, around the $(130)_\alpha$, and $(117)_\gamma$ reflections of the α and γ forms, respectively.[13,19] Moreover, the intensities and the positions of $(040)_\alpha$ and $(008)_\gamma$ reflection

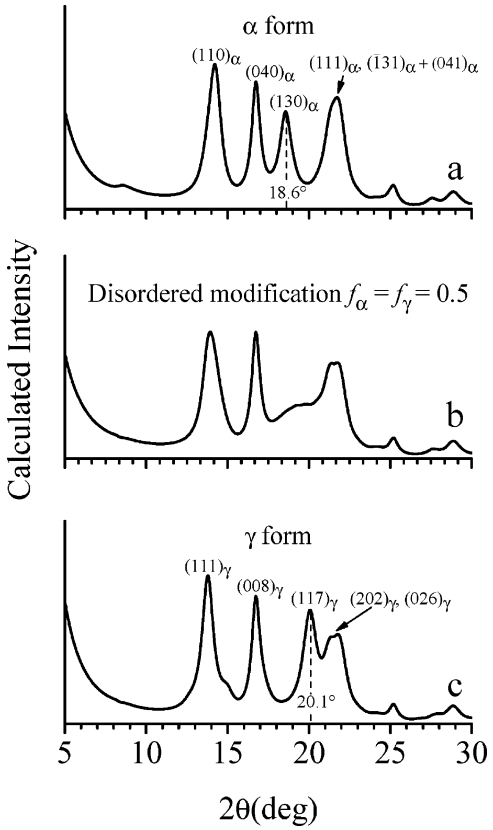

Figure 2. Calculated X-ray powder diffraction profiles of pure α (a) and γ (c) forms and of a disordered modification intermediate between the α and γ forms (b) including equal fractions of consecutive bilayers of chains stacked along b_α (c_γ) with the chain axes parallel, as in the α form (f_α), or nearly perpendicular, as in the γ form (f_γ), ($f_\alpha = f_\gamma = 0.5$).[13,19]

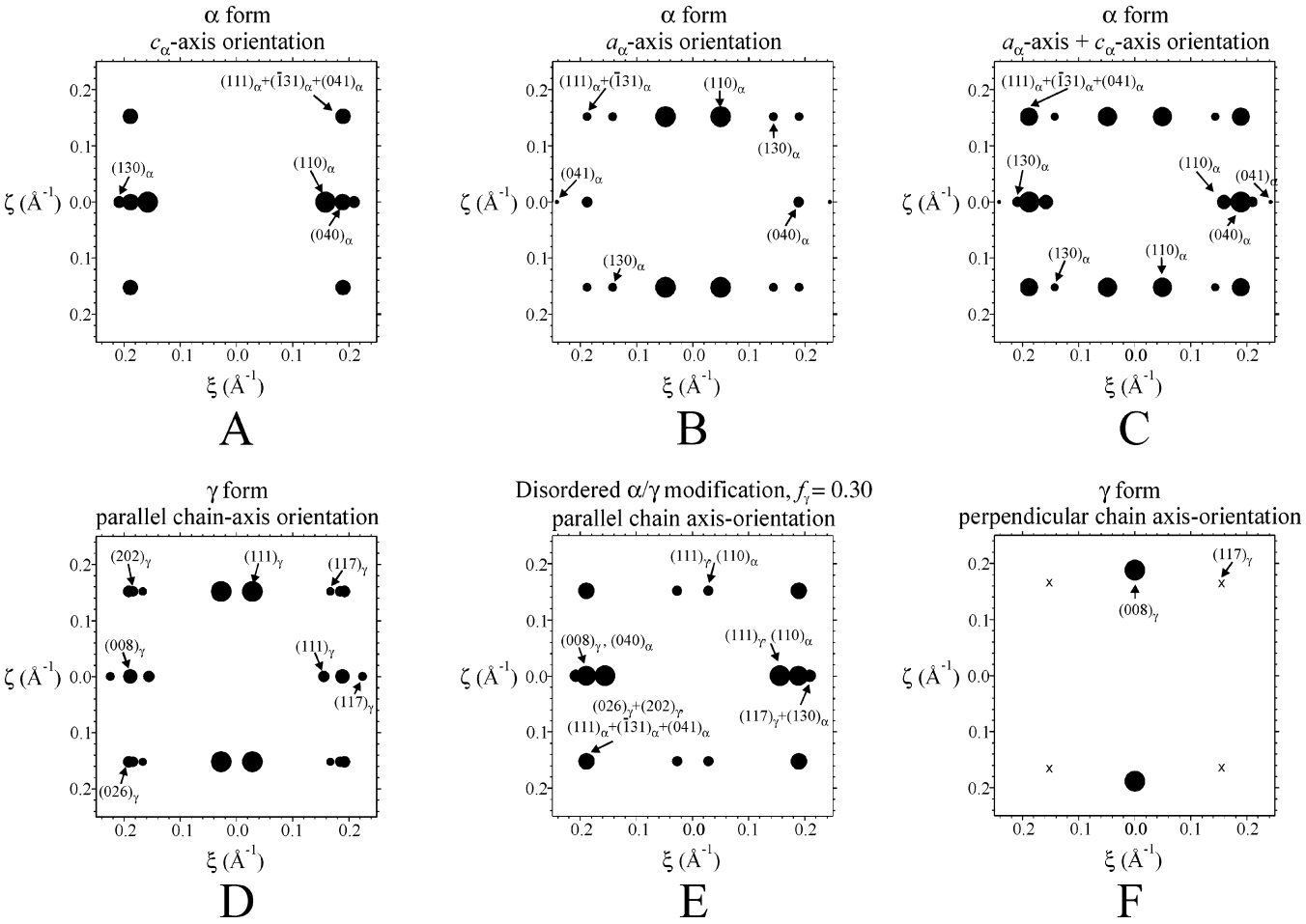

Figure 3. Calculated X-ray fiber diffraction patterns of iPP as a function of cylindrical reciprocal coordinates ξ and ζ for models of structures exhibiting limit kinds of preferred orientations. (A) α form with chain axes parallel to the fiber axis (c_α-axis orientation); (B) α form with a_α–axes parallel to the fiber axis (a_α-axis orientation); (C) α form with 50% crystals in the c_α-axis orientation, and 50% in a_α-axis orientation; (D) γ form with one-half of chain axes parallel to the stretching direction and the remaining portion of chains with axes tilted by ≈ 81° to the *z*-axis ("parallel chain axis orientation"); (E) a disordered modification intermediate between the α and γ forms, with $f_\gamma = 0.30$, in the "parallel chain axis orientation". The fraction of macromolecules with chain axes parallel to the fiber axis, $f_{||}$, is 0.85; (F) γ form with chain axes directed perpendicular to the fiber axis, i.e., with c_γ–axes oriented parallel to the fiber axis ("perpendicular chain axis orientation" or cross-β). The intensities of reflections are scaled with respect to the most intense reflection in each pattern, using balls of different diameters. In F, the intensity of $(117)_\gamma$ reflection, indicated with the symbol "X", is 1/32 the intensity of $(008)_\gamma$ reflection. Patterns similar to (F) (dominated by a single strong meridional refection at $\zeta \approx 0.19$ Å^{-1}) are calculated also in the case of domains of the α form and of α/γ disordered modifications with the direction of stacking of the bilayers of chains (b_α for the α form, c_γ for the γ form, see Figure 1) parallel to the fiber axis.

at $2\theta \approx 17°$ and of $(111)_\alpha$ and $(202)_\gamma$ reflection at $2\theta \approx 21°$ are not affected by the presence of α/γ disorder.[13,19] As shown in the X-ray diffraction profile of Figure 2b, the inclusion of a high degree of α/γ structural disorder in the crystalline domains ($f_\alpha = f_\gamma = 0.5$) implies that the $(130)_\alpha$ and $(117)_\gamma$ reflections are almost absent and only a diffuse scattering is observed in the corresponding 2θ range.

The stretching of samples of the α form generally induces preferential orientation of crystals with chain axes directed parallel to the stretching direction (c_α-axis orientation), like in a standard fiber morphology. However, in samples drawn at high temperature, lamellar branching may also occur.[36−39] Daughter lamellae grow on mother lamellae with the chain axes tilted ≈81° with respect to the chain axis of mother lamellae.[40] The contact faces between daughter and mother lamellae of the α form are the $a_\alpha - c_\alpha$ crystallographic planes (*B* face), and the tilting angle between the chain axes corresponds to the parameter $\beta_\alpha = 98.6°$ (i.e., 81°) of the monoclinic unit cell of the α form.[40] Therefore, while the mother lamellae are in the normal c_α-axis orientation, daughter lamellae present the a_α-axes directed parallel to the fiber axis (a_α-axis orientation). The origin of this lamellar branching is purely crystallographic and corresponds to a case of self-epitaxy that results from the near-identity of the a_α- and c_α-axes dimensions.[40] This kind of crosshatched morphology is typical of the α form crystallized from the melt or in oriented fibers, drawn at high temperatures.[36−39,41,42]

The calculated X-ray fiber diffraction patterns of fiber models of the α form in the c_α-axis orientation and in the a_α-axis orientation are reported in Figure 3A and B, respectively, as a function of cylindrical reciprocal coordinates ξ and ζ. It is apparent that, for crystals of the α form in the normal c_α-axis orientation, the $(110)_\alpha$, $(040)_\alpha$, and $(130)_\alpha$ reflections occur on the equator (at $2\theta \approx 14$, 17, and 18.6°, respectively), whereas the reflections $(111)_\alpha$ and $(\bar{1}31)_\alpha + (041)_\alpha$ are located on the first layer line at $2\theta \approx 21°$. For the tilted crystals of the α form in the a_α-axis orientation (Figure 3B), the $(110)_\alpha$ and $(130)_\alpha$ reflections disappear from the equator and appear on the first layer line, the $(041)_\alpha$ reflection becomes equatorial, whereas the positions of $(040)_\alpha$, $(111)_\alpha$, and $(\bar{1}31)_\alpha$ reflections are left unaltered in the same positions as those relative to the crystals of the α form with the normal c_α-axis orientation.

Of course, uniaxially drawn iPP samples in the α form containing a non-negligible fraction of tilted (daughter) lamellae aside mother lamellae with the normal c_α-axis orientation present

X-ray fiber diffraction patterns having features intermediate between those of Figure 3A and B. The calculated X-ray fiber diffraction pattern for a fiber model containing equal proportions of mother and daughter lamellae is shown in Figure 3C. The $(110)_\alpha$, $(130)_\alpha$, and $(041)_\alpha$ reflections appear both on the equator and on the first layer line, the $(040)_\alpha$ lays on the equator, and the $(111)_\alpha$ and $(\bar{1}31)_\alpha$ reflections are placed on the first layer line (Figure 3C).

The oriented γ form was early obtained by Awaya in the case of a thin film of a low-molecular-weight iPP sample, prepared by melt crystallization.[43] The strong analogies between the X-ray diffraction patterns of oriented specimens of iPP in the γ form and those of uniaxially oriented samples of iPP crystallized in the α form affected by lamellar branching was already pointed out by Awaya.[43] The only marked difference is, indeed, in the 2θ position of a strong reflection, located on the equator and the first layer line at $2\theta \approx 20°$ for the γ form ($(117)_\gamma$ reflection) instead of $2\theta = 18.6°$ for the α form ($(130)_\alpha$ reflection).[43] The crystal structure of the γ form[29] had not yet been solved at that time. The quantitative analysis of the diffraction pattern of the oriented γ form could be performed only recently, in the case of stretched fibers of a high molecular weight, poorly isotactic polypropylene sample,[13] presenting a diffraction pattern similar to that of ref 43. In this sample, crystals of the γ form tend to assume a preferred orientation with one half of chain axes parallel to the stretching direction and the second half of chains directed at an angle of $\approx 81°$ with respect to the fiber axis. We define this preferential orientation as "parallel chain axis orientation".[13] This kind of preferential orientation of crystals of the γ form has been observed in samples of commercial iPP obtained by shear-controlled orientation injection molding (SCORIM) technique[7] and in pitch-based carbon or Kevlar fiber-reinforced composites as a result of crystallization of iPP on the surface of the fibers.[34]

The calculated X-ray fiber diffraction pattern for a fiber model of the γ form in the parallel chain axis orientation is schematically shown in Figure 3D. The $(111)_\gamma$ and $(117)_\gamma$ reflections at $2\theta \approx 14$ and 20°, respectively, appear both on the equator and the first layer line, the $(008)_\gamma$ reflection at $2\theta \approx 17°$ appears on the equator, whereas the $(202)_\gamma$ and $(026)_\gamma$ reflections at $2\theta \approx 21°$ are located on the first layer line. It is apparent that the X-ray fiber diffraction patterns of the oriented γ form with parallel chain axis orientation, shown in Figure 3D, presents noticeable analogies with the X-ray diffraction patterns of fibers of the α form affected by lamellar branching, shown in Figure 3C. The most remarkable differences are in the position of the third strong equatorial reflection, at $\xi \approx 0.21$ Å^{-1} in the pattern of Figure 3C of the α form ($(130)_\alpha$ reflection at $2\theta \approx 18.6°$) and at $\xi = 0.23$ Å^{-1} in the pattern of Figure 3D of the γ form ($(117)_\gamma$ reflection at $2\theta \approx 20.1°$), and in the ξ positions on the first layer line of the $(110)_\alpha$ reflection of the α form ($\xi \approx 0.043$ Å^{-1}, $2\theta \approx 14°$, Figure 3C) and $(111)_\gamma$ reflection of the γ form ($\xi \approx 0.030$ Å^{-1}, $2\theta \approx 14°$, Figure 3D).

The calculated X-ray fiber diffraction pattern for a fiber model with crystals in a disordered modification intermediate between the α and γ forms (Figure 1B), oriented according to the parallel chain axis orientation, is shown in Figure 3E. The diffraction intensity distribution depends on the fraction of consecutive bilayers facing as in the γ form (f_γ) and on the fraction of bilayers with chain axes aligned parallel to the fiber axis ($f_{||}$). The case with $f_\gamma = 0.3$ and $f_{||} = 0.85$ is shown in Figure 3E as an example. The $(111)_\gamma$ reflection of the γ form ($(110)_\alpha$ reflection for the α form at $2\theta = 14°$) is split in an equatorial and a first layer line component, as in the pure γ form (Figure 3D), but at variance with the pure γ form, the intensity of the first layer line component is much lower than the intensity of the equatorial component (Figure 3E). The $(117)_\gamma$ reflection ($2\theta \approx 20°$) of the γ form is absent, but a broad peak is now apparent on the equator at $2\theta \approx 18.6°$, corresponding to the $(130)_\alpha$ refection of the α form. The intensity of the $(130)_\alpha$ reflection is unusually low with respect to the intensity of the $(040)_\alpha$ reflection at $2\theta \approx 17°$. As in the pure γ form, the $(008)_\gamma$ reflection of the γ form ($(040)_\alpha$ reflection of the α form at $2\theta \approx 17°$) is located on the equator, whereas the $(202)_\gamma$ and $(026)_\gamma$ reflections of the γ form ($(111)_\alpha$ and $(\bar{1}31)_\alpha$ reflections for the α form) and the $(041)_\alpha$ reflection of the α form (at $2\theta \approx 21°$) are located on the first layer line.

Therefore, in an experimental X-ray fiber diffraction pattern, the presence of a broad and weak reflection on the equator in the 2θ region 18−20°, associated with a small, if any, polarization of the reflection at $2\theta = 14°$ ($(111)_\gamma$ reflection for the γ form or $(110)_\alpha$ reflection for the α form) on the first layer line, besides the presence of strong diffraction peaks at $2\theta \approx 14$ and 17° ($(110)_\alpha$ or $(111)_\gamma$ and $(040)_\alpha$ or $(008)_\gamma$ reflections, respectively) on the equator and at $2\theta \approx 21°$ on the first layer line, indicates that the crystals present a high degree of α/γ disorder (Figure 1B) that includes a prevalent fraction of adjacent bilayers faced as in the α form ($f_\gamma < 0.5$), with the chain axes parallel to the fiber axis ($f_{||} > 0.5$).

A different kind of preferred orientation that crystals of the γ form may assume at low and moderate deformations consists of the alignment of the c_γ-axis (that is the direction of stacking of bilayers of chains, see Figure 1C) parallel to the stretching direction (fiber axis) and, therefore, with the two sets of chain axes directed along directions nearly normal to the stretching direction. We define this preferential orientation "perpendicular chain axis orientation".[14,16] A similar kind of orientation has been well-known for many years in some naturally occurring fibrous proteins such as silks.[44] The perpendicular orientation of chain axes with respect to the fiber axis, described as "cross-β", occurs at low draw ratio and has been explained by the fact that in these soft silks the small crystallites are elongated along the hydrogen bond directions, which run perpendicular to chain axes.[44] In the case of iPP, this nonstandard mode of orientation of polymer crystals has been observed also in the case of iPP composites reinforced with polyacrylonitrile-based carbon fibers and arises from restriction of isotropic growth of α crystallites by the presence in the polymer matrix of unidirectionally placed carbon fibers.[34]

The calculated X-ray diffraction pattern for a fiber model, presenting γ crystals oriented with the c_γ-axes parallel to the fiber axis (perpendicular chain axis orientation or cross-β), is schematically shown in Figure 3F as a function of cylindrical reciprocal coordinates ξ and ζ. This pattern is characterized by the presence of a strong meridional spot at $2\theta \approx 17°$, corresponding to the $(008)_\gamma$ reflection. The remaining reflections of the γ form appear of low intensity. The symbol "X" in Figure 3F indicates the position of the second strongest intensity reflection for this limit mode of preferred orientation and corresponds to the $(117)_\gamma$ reflection of the γ form at $2\theta \approx 20°$. In this orientation, the intensity of the $(117)_\gamma$ reflection is 1/32 of the intensity of the $(008)_\gamma$ reflection. It is worth noting that analogous patterns would be calculated also in the case of crystals of the α form or in α/γ disordered modifications of the kind shown in Figure 1B, oriented in the perpendicular chain axis orientation. Also, in these cases, indeed, the diffraction pattern would be dominated by the presence of a strong meridional reflection at $\zeta \approx 0.19$ Å^{-1}, corresponding to the

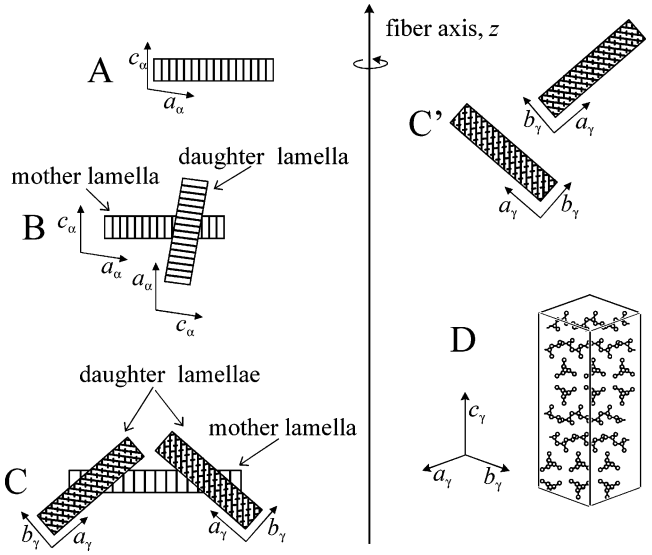

Figure 4. Limit preferential orientations of iPP crystals of the α and γ forms (or of α/γ disordered modifications) in stretched fibers. The fiber axis is labeled with *z*. The chain axes are indicated with straight lines. (A) Lamella of the α form oriented with chain axes directed parallel to the fiber axis (c_α-axis orientation). (B) Daughter lamella of the α form oriented with chain axes tilted by ≈81° to the fiber axis (a_α-axis orientation) grown by epitaxy on a mother lamella of the α form in the normal c_α-axis orientation. (C, C′) Crystals of the γ form (or of α/γ disordered modifications) oriented with portion of chain axes parallel to the fiber axis, so that the remaining portion of chains have the axes tilted by ≈81° to the *z*-axis ("parallel chain axis orientation"). In C, the γ lamellae are grown by epitaxy on a mother lamella of the α form in the normal c_α-axis orientation. (D) Crystal of the γ form oriented with the bilayers of chains perpendicular to the fiber axis and, therefore, with the direction of stacking of bilayers of chains, the c_γ-axis, parallel to the *z*-axis and the chain axes perpendicular to the fiber axis ("perpendicular chain axis orientation" or "cross-β").

$(040)_\alpha$ reflection of the α form and the $(008)_\gamma$ reflection of the γ form, and only a negligible intensity for all remaining reflections. Therefore, in an experimental X-ray fiber diffraction pattern, the presence at $2\theta \approx 17°$ of intensity maximum on the meridian or in a nearly meridional position indicates the presence of crystalline domains (in the α and γ forms or in a disordered α/γ modification) oriented according to the perpendicular or nearly perpendicular chain axis orientation (cross-β).

The limit preferential orientations that crystals of the α and/or γ forms (or of α/γ disordered modifications) may assume by uniaxial drawing are sketched in Figure 4. The lamellae appear as elongated entities of lateral dimensions larger than the thickness. The chain axes (indicated with straight lines) run perpendicular to the basal plane of the lamellae of the α form (Figure 4A) and tilted by ≈40° to the basal plane of lamellae of the γ form (Figure 4C). The case of lamellae of the γ form in the "parallel chain axis orientation" is illustrated in Figure 4C′, whereas two cases of lamellar branching are shown in Figure 4B,C. In Figure 4B, lamellar branching occurs between two lamellae of the α form: the mother lamella is oriented in the normal c_α-axis orientation, whereas the daughter lamella is in the a_α-axis orientation. In Figure 4C, a mother lamella of the α form is shown in the normal c_α-axis orientation, along with two lamellae of the γ form grown by epitaxy in the "parallel chain axis orientation". As shown by Lotz et al.,[45] the α phase may nucleate the growth of daughter lamellae in the α or γ forms; the γ form, in turn, may nucleate epitaxial growth of the α form, but not of the γ form. The "perpendicular chain axis orientation" or "cross-β" is illustrated in Figure 4D in the case of a lamella of the γ form. The direction of stacking of bilayers of chains, the c_γ-axis, is oriented parallel to the fiber axis and the chain axes are oriented along directions perpendicular to the fiber axis.

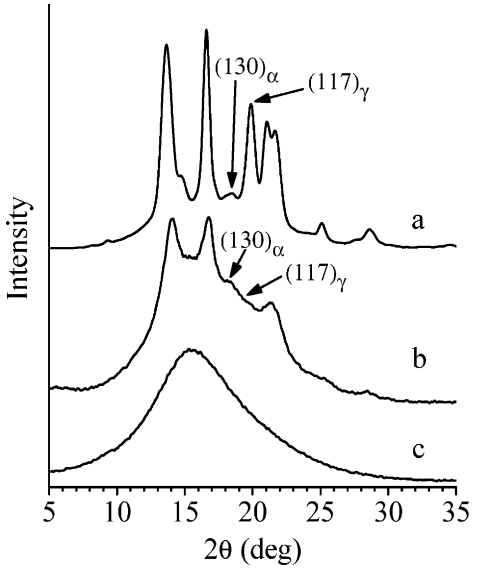

Figure 5. X-ray powder diffraction profiles of melt-crystallized compression molded films of the sample R (a) and of fractions W(HS) (b) and W(ES) (c) of the sample W. The $(130)_\alpha$ reflection typical of the α form at $2\theta = 18.6°$ and $(117)_\gamma$ reflection typical of the γ form at $2\theta = 20.1°$ are indicated.

Results and Discussion

Unoriented Samples. The X-ray powder diffraction profiles of unoriented films of samples R, W(HS), and W(ES) obtained by compression molding, used as starting materials of our analysis, are shown in Figure 5.

The diffraction profile of sample R (Figure 5a) indicates that this sample develops a high degree of crystallinity from the melt, corresponding to 66%. The presence of strong $(111)_\gamma$, $(008)_\gamma$, $(117)_\gamma$, and $(202)_\gamma + (026)_\gamma$ reflections at $2\theta \approx 14$, 17, 20, and 21°, respectively, typical of the γ form and the low intensity of $(130)_\alpha$ reflection at $2\theta \approx 18.6°$, typical of the α form (Figure 5a), indicates that sample R is basically in the γ form, in mixture with a small amount of crystals in the α form.

The diffraction profile of the fraction W(HS) (Figure 5b) indicates a low degree of crystallinity, corresponding to ≈41% and is characterized by the presence of only three reflections at $2\theta = 14$, 17, and 21°. The absence of the $(117)_\gamma$ reflection of the γ form at $2\theta = 20.1°$ and the presence of only a small diffraction peak at $2\theta = 18.6°$ corresponding to the $(130)_\alpha$ reflection of the α form in the profile of Figure 5b indicate that the crystalline phase of the sample W(HS) is characterized by α/γ disordered modifications of the kind shown in Figure 1B, with only a slight prevalence of consecutive bilayers faced as in the α form (compare the pattern of Figure 5b with the calculated pattern of Figure 2b).[20]

The diffraction pattern of the fraction W(ES) (Figure 5c) presents only a broad halo, indicating that this fraction is amorphous.[20]

Oriented Fibers: Sample R. The structural transformations that occur upon stretching iPP samples initially in the pure γ form have been described in a recent paper in the case of metallocene-made iPP samples having microstructure similar to that of the sample R, but higher content of *rr* stereodefects and higher molecular mass.[16]

The X-ray fiber diffraction patterns, and the corresponding profiles read along the equatorial line, of fibers of the sample R obtained by stretching at room-temperature compression

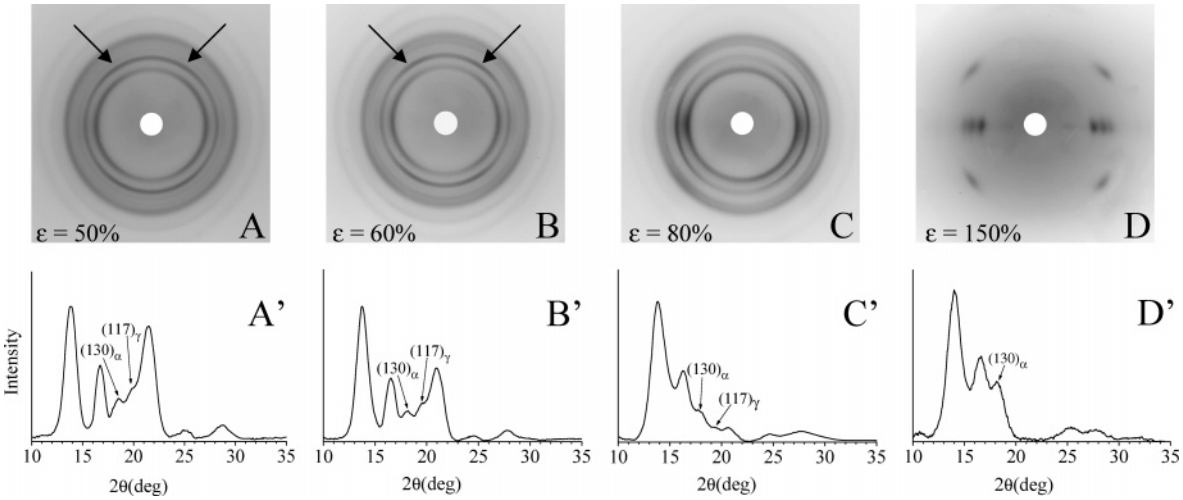

Figure 6. X-ray fiber diffraction patterns (A−D), and corresponding equatorial profiles (A′−D′), of fibers of the sample R obtained by stretching at room-temperature compression molded films at values of strain ϵ of 50% (A), 60% (B), 80% (C), and 150% (D). The equatorial profiles (A′−D′) have been subtracted for the background intensity and the contribution of the amorphous phase. The $(130)_\alpha$ and $(117)_\gamma$ reflections typical of the α and γ forms at $2\theta = 18.6$ and 20°, respectively, are indicated. In A and B, the off-equatorial polarization of the reflection at $2\theta \approx 17°$ ($(040)_\alpha$ reflection of the α form and $(008)_\gamma$ reflection of the γ form) is indicated with arrows.

molded films at different values of the strain ϵ are reported in Figure 6. The γ form present in the initial unoriented film (Figure 5a) gradually transforms into the α form through a continuum of α/γ disordered modifications (Figure 6). At 50% deformation, the crystals are poorly oriented (Figure 6A). Moreover, the absence of the $(117)_\gamma$ reflection of the γ form at $2\theta = 20.1°$ and the presence of the $(130)_\alpha$ reflection of the α form at $2\theta = 18.6°$ of small intensity (Figure 6A′) indicate that the γ form, originally present in the sample, transforms, already at this low deformation, into α/γ disordered modifications, where the fraction of consecutive bilayers of chains facing as in the α form is prevalent over that of bilayers facing as in the pure γ form ($f_\gamma < 0.5$).

The degree of orientation of crystals increases with increasing deformation ($\epsilon > 50\%$), as indicated by the increase of the polarization of reflections at $2\theta \approx 14$, 17, and 18.6° on the equator in the diffraction patterns of Figure 6B−D. Moreover, the intensity of the $(130)_\alpha$ reflection at $2\theta \approx 18.6°$ increases (Figure 6B′−D′). This indicates that the relative amount of consecutive bilayers faced as in the γ form (f_γ) decreases, whereas the fraction of consecutive bilayers faced as in the α form (f_α) increases with increasing deformation. At the maximum possible deformation ($\epsilon = 150\%$), the fiber is basically in the α form with c_α-axis orientation (Figure 6D) and a high degree of orientation of the crystals is achieved. The equatorial profile (Figure 6D′) presents, indeed, the three strong $(110)_\alpha$, $(040)_\alpha$, and $(130)_\alpha$ equatorial reflections at $2\theta = 14$, 17, and 18.6°, typical of the α form. A broad halo subtending the Bragg's reflections is also present, indicating a partial formation of the mesomorphic form of iPP at high deformation. These data show that crystals of the γ form initially present in the sample transform into the α form or in α/γ disordered modifications, more similar to the α form by stretching. At high deformation, the α form, in turn, partially transforms into the mesomorphic form. However, at variance with samples analyzed in ref 16, the pure mesomorphic form is not obtained due to the fact that the low molecular mass of sample R prevents stretching the sample at deformations higher than 150%.

The transformation of the γ form into the α form and/or into α/γ disordered modifications closer to the α form cannot be direct and probably occurs via the pulling out of chains from the original γ crystals upon application of the tensile stress, followed by recrystallization in fibrillar crystals of lateral size smaller than that of crystals originally present in the material, with chain axes directed along the stretching direction. In particular, using the Scherrer formula, the average dimensions of crystallites along the direction perpendicular to $(040)_\alpha$ planes of the α form or $(008)_\gamma$ planes of the γ form, correspond to nearly 90 Å at 50% deformation and decrease by ≈33% at 150% deformation. Direct transformation of the γ form into the α form is prevented for steric reasons by the fact that, whereas in the γ form the bilayers of chains are stacked along the c_γ-axis direction according to the sequence ...LRRLLR... (Figure 1C),[29] in the α form the bilayers are stacked along the b_α-axis direction with a strict alternation of helical hands ...LRLRLR... (Figure 1A).[30] This transformation would imply simultaneous inversion of the helical hand of the chains belonging to every bilayer, making a direct mechanism very unlikely.

In summary, the data of Figures 6 indicate that the structural transformation of the γ form into the α form occurs gradually with increasing deformation and involves the formation of α/γ disordered modifications, where the relative amount of bilayer of chains arranged with parallel chain axes as in the α form, f_α, increases, whereas the fraction of bilayers arranged with perpendicular chain axes as in the γ form, f_γ, decreases.

Moreover, the morphological transformation from randomly oriented crystals (probably spherulitic morphology) into the fibrillar morphology of sample R is also gradual and, at low deformations ($\epsilon < 80\%$), a nonstandard mode of preferred orientation of iPP crystals occurs. In fact, portion of the crystals of the γ form, or in α/γ disordered modifications more similar to the γ form, assumes at low deformations an orientation with the c_γ-axes of the γ form (b_α-axes of the α form) nearly parallel to the stretching direction, as indicated by the nearly meridional polarization of the $(008)_\gamma$ reflection of the γ form (or $(040)_\alpha$ reflection of the α form) at $2\theta = 17°$ in the patterns of Figure 6A,B. Because the c_γ-axes of the γ form (b_α-axes of the α form) are the axes of stacking of bilayers of chains (Figure 1), this nonstandard mode of orientation of iPP crystals corresponds to lamellae oriented with chain axes nearly perpendicular to the fiber axis (cross-β or perpendicular chain axis orientation, Figure 3F). The cross-β orientation may be attributed to the simultaneous occurrence of two kinds of slip processes at low deformations, interlamellar and intralamellar.[46] Interlamellar

shear leads to a location of the $(008)_\gamma$ reflection of the γ form ($(040)_\alpha$ reflection of the α form) on the meridian, whereas the intralamellar shear pushes the chain axes to align parallel to the stretching direction and thus shifts the position of the reflection at $2\theta = 17°$ toward the equator.

These data support the hypothesis that not all the crystals of the γ form originally present in the sample experience simultaneously the uniaxial mechanical stress field, and the nonstandard mode of orientation of these crystals reflects crystallographic restraints on the slip processes and topological constraints on the response of crystals to the tensile stress field. In the crystalline domains of the γ form, indeed, the chains are oriented along two perpendicular directions, and the crystallites have the shape of elongated entities along the direction normal to the chain axes.[16] Because of the intrinsic structural and morphological features of the γ form, at low deformations, a portion of the γ crystals remains frozen in strained positions of the polymer matrix with the chain axes oriented nearly perpendicular to the stretching direction. By stretching at higher deformations, the γ form transforms into the α form. Because in the α form the chains are all parallel, the deformation also induces orientation of crystals with the chain axes oriented along the stretching direction, as in a standard fiber morphology (c_α-axis orientation).

Oriented Fibers: Sample W(HS). The sample W(HS) is characterized by chains with an isotactic and atactic stereoblock structure and presents interesting elastomeric behavior in a wide range of deformations.[9,10] As shown in Figure 5b, crystals of the initial melt-crystallized unstretched sample, obtained by compression molding, are in α/γ disordered modifications.[20] The X-ray fiber diffraction patterns of the sample W(HS) and the corresponding equatorial profiles, obtained by stretching compression molded films at values of strain ϵ of 200, 500, and 700%, and after releasing the tension, are reported in Figure 7.

The diffraction pattern of the fiber stretched at $\epsilon = 200\%$ (Figure 7A) presents reflections at $2\theta \approx 14$ and 17° slightly polarized on the equator, with a low degree of orientation of the crystals. The absence of the $(117)_\gamma$ reflection of the γ form at $2\theta \approx 20°$ and the presence of the $(130)_\alpha$ reflection of the α form at $2\theta = 18.6°$ of low intensity in the equatorial profile of Figure 7A′ indicate that the fiber is characterized by α/γ disordered modifications, as in the unstretched sample, with only a small increase of the fraction of consecutive bilayers of chains faced as in the α form with parallel chains. Therefore, at low deformation ($\epsilon = 200\%$), a fraction of the original crystals in α/γ disordered modifications with a slightly prevalent fraction of bilayers of chains faced as in the α form, present in the unoriented film (Figure 5b), transforms by stretching into modifications closer to the α form in the parallel chain axis orientation.

The X-ray diffraction pattern of the stress-relaxed fiber obtained by removing the tension from 200% strain (fiber W(HS)-200, Figure 7B,B′) presents two strong diffraction rings at $2\theta \approx 14$ and 17° slightly polarized on the equator, and a ring at $2\theta \approx 21°$, slightly polarized on the first layer line. At variance with the equatorial profile of the corresponding stretched fiber of Figure 7A′, the $(130)_\alpha$ reflection of the α form at $2\theta = 18.6°$ and the $(117)_\gamma$ reflection of the γ form at $2\theta = 20.1°$ are both present in the equatorial profile of the stress-relaxed fiber W(HS)-200 (Figure 7B′). The small and almost identical intensities of these two reflections indicate that the stress-relaxed fiber W(HS)-200 is characterized by the presence of two families of crystals in α/γ disordered modifications in a nearly 1:1 ratio. A portion of crystals is in disordered modifica-

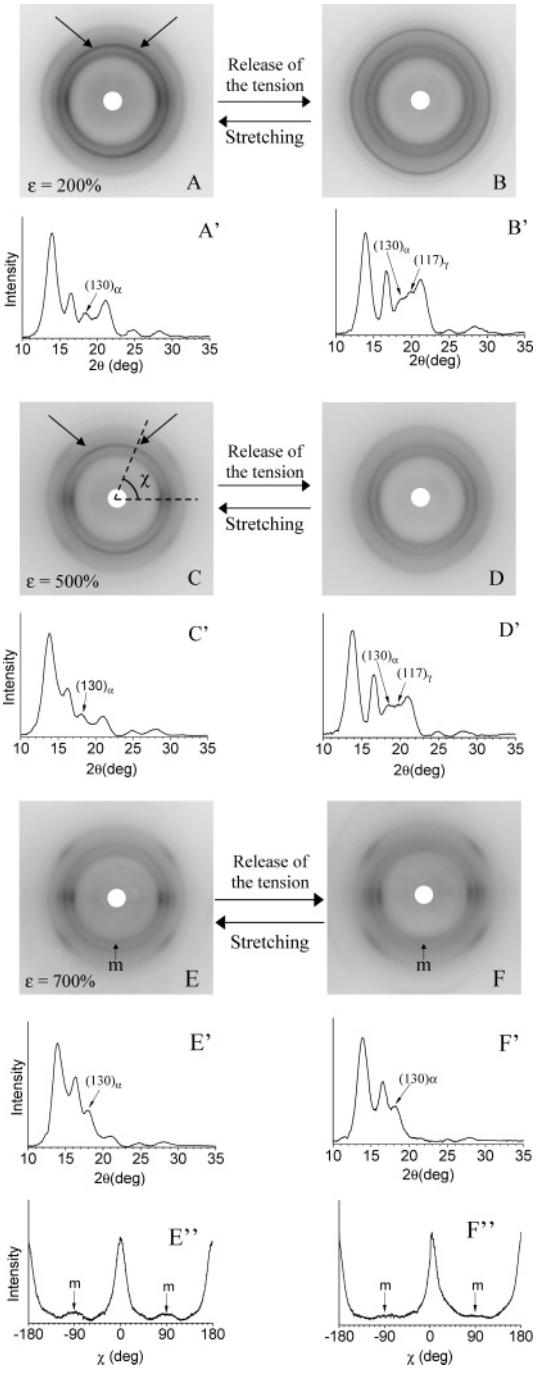

Figure 7. X-ray fiber diffraction patterns (A−F) and corresponding profiles read along the equatorial lines (A′−F′) of fibers of the sample W(HS), obtained by stretching compression molded films at the indicated values of strain (A, C, E) and after removing the tension (B, D, F). The azimuthal angle χ of the reflection at $2\theta \approx 17°$, indicated by arrows in (A) and (C), is defined in (C). For the fiber stretched at 700% deformation, the diffraction profile read along the azimuthal arc χ of the $(110)_\alpha$ or $(111)_\gamma$ reflection at $2\theta \approx 14°$ is also reported for the stretched fiber (E″) and after removing the tension (F″). The equatorial profiles (A′−F′) have been subtracted for the background intensity and the contribution of the amorphous phase. The $(130)_\alpha$ reflection of the α form and the $(117)_\gamma$ reflection of the γ form, at $2\theta = 18.6$ and 20°, respectively, are indicated. The reflections labeled with "m" in E, E″, F, and F″ indicates the nearly meridional component of $(111)_\gamma$ reflection due to lamellae of the γ form oriented with chain axes parallel to the stretching direction (Figures 3D and 4C′) and/or the meridional component of the $(110)_\alpha$ reflection of the α form, or of $(111)_\gamma$ reflection of the γ form (Figure 3C) due to the presence of a nonnegligible amount of daughter lamellae of α or γ form tilted ≈81° with respect to the parent lamellae (Figure 4B,C, crosshatch).[37−40,13]

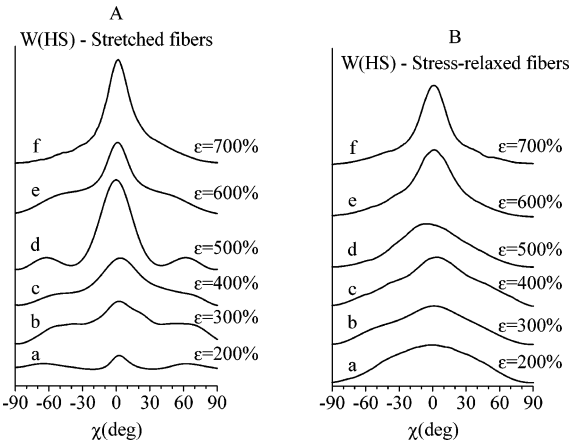

Figure 8. X-ray diffraction azimuthal profiles of the reflection at $2\theta = 17°$ in the X-ray fiber diffraction patterns of sample W(HS) stretched at the indicated values of deformation (Figure 7). The azimuthal scans are reported for fibers obtained by stretching compression molded films at the indicated elongation, keeping the fiber under tension (A) and after removing the tension (B).

tions closer to the α form with a higher fraction of bilayers facing with parallel chains ($f_\gamma < 0.5$), and the other portion of crystals is in modifications closer to the γ form with a higher fraction of bilayers of chains facing with perpendicular chains ($f_\gamma > 0.5$). Furthermore, the (low) degree of orientation of the crystalline phase achieved in the stretched fiber (Figure 7A) decreases upon releasing the tension (Figure 7B).

The most remarkable difference between the diffraction patterns of the W(HS) fiber stretched at $\epsilon = 200\%$ (Figure 7A) and the stress-relaxed fiber W(HS)-200 (Figure 7B) is in the distribution of intensity of the $(008)_\gamma$ reflection of the γ form ($(040)_\alpha$ reflection of the α form) at $2\theta \approx 17°$, along the azimuthal arc χ, defined in Figure 7C ($\chi = 0$ and 90° for equatorial and meridional reflections, respectively). The azimuthal profiles of the reflection at $2\theta \approx 17°$ in the X-ray fiber diffraction patterns of sample W(HS) stretched at different values of deformation, and of the corresponding stress-relaxed fibers, are compared in Figure 8.

It is apparent that, in the case of the sample W(HS) stretched at 200% deformation, the reflection at $2\theta \approx 17°$ appears slightly polarized on the equator ($\chi = 0$) and in positions close to the meridian at $\chi \approx \pm 60°$ (Figure 8A, curve a). After releasing the tension, the distribution of intensity of this reflection becomes more uniform, with only a broad maximum centered on the equator (Figure 8B, curve a). This possibly indicates that, in the stretched sample, a non-negligible portion of crystals in disordered modifications closer to the γ form, originally present in the unstretched film, are frozen in strained positions of the polymer matrix with the c_γ-axis (b_α-axis) inclined at ≈30° to the stretching direction, in the cross-β orientation (or perpendicular chain axis orientation, Figure 4D). These crystals return back in the isotropic matrix, loosing this preferred cross-β orientation by releasing the tension, assuming less strained orientations in the polymer network, and the overall degree of orientation of crystals decreases (Figure 7B). Crystals that experience this reorientation process are probably in α/γ disordered modifications closer to the γ form, with a higher fraction of bilayers facing with perpendicular chains, as indicated by the fact that the $(117)_\gamma$ reflection of the γ form is absent in the X-ray fiber diffraction pattern of Figure 7A′ of the stretched sample (this reflection is absent when crystals of γ form are in cross-β orientation, see Figure 3F) and is present in the X-ray fiber diffraction pattern of the stress-relaxed fiber W(HS)-200 (Figure 7B′).

The data of Figure 7A,B indicate that structural and morphological transformations occur during stretching and relaxation. During stretching, the portion of crystals originally in disordered modifications closer to the γ form, present in the unstretched film, transform into disordered modifications closer to the α form in the parallel chain axis orientation. Another portion of the original crystals remains in disordered modifications closer to the γ form but assume the cross-β orientation. These crystals in cross-β orientation return back into the isotropic matrix, without retaining preferential orientation after removing the tension. Crystals of the α form, formed during stretching, instead, remain in the parallel chain axis orientation after releasing the tension. The flip−flop textural transformation involving crystals in cross-β orientation is reversible during mechanical cycles of stretching (up to the maximum length, $3L_0$, achieved during stretching of the unoriented sample), followed by relaxation upon releasing the tension. The elastic recovery is almost complete during these cycles.[10] In particular, the residual deformation of unoriented compression-molded films of the sample W(HS) stretched at 200% deformation and then stress-relaxed is 38%, whereas stress-relaxed fibers, prepared by stretching the compression molded films up to 200% deformation, keeping the fibers under tension for 10 min at room temperature, then removing the tension, allowing the specimens to relax, show a residual deformation below 2%.

The degree of orientation of crystals in the "parallel chain axis orientation" increases with increasing deformation. In the X-ray diffraction pattern of the sample W(HS) stretched at 500% deformation (Figure 7C), indeed, the reflections at $2\theta \approx 14°$ ($(111)_\gamma$ of the γ form and $(110)_\alpha$ of the α form) and 17° ($(008)_\gamma$ of the γ form and $(040)_\alpha$ of the α form) are more polarized on the equator, whereas the reflections at $2\theta \approx 21°$ ($(202)_\gamma$ and $(026)_\gamma$ reflections of the γ form, $(111)_\alpha$, and $(\bar{1}31)_\alpha + (041)_\alpha$ reflections of the α form) are polarized on the first layer line.

It is worth noting that also at $\epsilon = 500\%$, the reflection at $2\theta \approx 17°$ ($(008)_\gamma$ of the γ form and $(040)_\alpha$ of the α form) results polarized not only on the equator (at $\chi = 0$) but also in positions close to the meridian, at $\chi \approx \pm 60$ (Figure 7C and curve d of Figure 8A). The orientation of the crystals in this sample is therefore bimodal, that is, a portion of crystals is oriented in the parallel chain axis orientation ($\chi = 0$), and the other portion in the nearly perpendicular chain axis orientation or cross-β ($\chi \approx \pm 60°$).

The stress-relaxed fiber obtained from the fiber of the sample W(HS) stretched at 500% after removing the tension (fiber W(HS)-500%) has a lower degree of orientation of crystals, as indicated by the fact that the intensity distribution along χ of the reflections at $2\theta \approx 14$ and 17° becomes more uniform (Figure 7D and curve d of Figure 8B). As in the case of the stress-relaxed fiber W(HS)-200, also in the equatorial profile of the stress-relaxed fiber W(HS)-500 (Figure 7D′), the $(130)_\alpha$ reflection of α the form at $2\theta = 18.6°$ and the $(117)_\gamma$ reflection of the γ form at $2\theta \approx 20°$ are both present, and the intensity of the $(117)_\gamma$ reflection increases with respect to that of the stretched fiber (Figure 7C′); furthermore, the reflection at $2\theta \approx 17°$ becomes polarized exclusively on the equator (curve d of Figure 8B). This indicates a change of texture from cross-β to isotropic orientation upon releasing the tension.

In summary, crystals in α/γ disordered modifications more similar to the γ form, originally present in the unoriented film, gradually transform by stretching into modifications closer to the α form. Because these crystals have a high fraction of chains with parallel chain axes, they are easily oriented in the parallel chain axis orientation, and their degree of orientation increases

with increasing deformation. Furthermore, at low and moderate deformations, fibers of the sample W(HS) are characterized by the presence of a nearly 1:1 mixture of crystals in α/γ disordered modifications characterized by a different proportion of consecutive bilayers of chains faced as in the γ form, a portion of crystals being in disordered modifications closer to the α form ($f_\gamma < 0.5$), and the other portion of crystals in modifications closer to the γ form ($f_\gamma > 0.5$). In the fibers stretched at 200 and 500% deformations, the portion of crystals in disordered modifications closer to the α form are oriented in the parallel chain axis orientation, whereas the portion of crystals in disordered modifications closer to the γ form are oriented in the cross-β orientation (or perpendicular chain axis orientation). Upon releasing the tension, crystals in cross-β orientation, which are in strained positions of the polymer network, return to less strained and random positions, whereas crystals with parallel chain axis orientation remain almost unaffected, with the result that the degree of orientation of the crystals in the parallel chain axis orientation achieved in the stretched fiber is partially lost. The elastic properties for the fraction W(HS) in a large deformation range[10] are probably due to the fact that these flip−flop textural transformations of the crystalline phase are reversible so that unoriented films undergo small plastic deformation by stretching at these deformations during the irreversible transformations from spherulitic to fibrillar morphology.

Finally, the X-ray fiber diffraction patterns of the sample W(HS) stretched at 700% deformation (Figure 7E,E′) presents maxima at $2\theta \approx 14$, 17, and 18.6° ($(110)_\alpha$, $(040)_\alpha$, and $(130)_\alpha$ reflections, respectively) on the equator, and at $2\theta \approx 21°$ ($(111)_\alpha + (\bar{1}31)_\alpha + (041)_\alpha$ reflections) on the first layer line, without any appreciable polarization of the reflection at $2\theta \approx 17°$ in positions close to the meridian (Figures 7E and curve f of Figure 8A). Moreover, the reflection $(117)_\gamma$ at $2\theta \approx 20°$ is completely absent. This indicates that crystals originally in α/γ disordered modifications closer to the γ form transform into modifications more similar to the α form at high draw ratios, including only a small amount, if any, of α/γ structural disorder. These crystals achieve a high degree of orientation in the normal c_α-axis orientation as in a standard fiber orientation; there is no evidence of the presence of crystals in the nearly perpendicular chain axis orientation.

It is worth noting that, in the diffraction pattern of the sample W(HS) stretched at $\epsilon = 700\%$ (Figure 7E), the $(110)_\alpha$ reflection at $2\theta \approx 14°$ presents maxima not only on the equator (at $\chi = 0$) but also in positions close to the meridian (at $\chi = \pm 90°$), indicated with the symbol "m" in Figure 7E. The intensity of the $(110)_\alpha$ reflection at $2\theta \approx 14°$ along the azimuthal arc χ is shown in Figure 7E″. As shown in the previous section (Figure 3), the presence of the $(110)_\alpha$ reflection on the meridian ($\chi \approx 90°$ in Figure 7E″) may originate from the presence of a nonnegligible portion of daughter lamellae, tilted by ≈81° with respect to the parent lamellae, the latter being oriented with the chain axes parallel to the stretching direction. The daughter lamellae grow up by epitaxy on the α lamellae formed by stretching at high draw ratios, creating a crosshatched morphology. Because of the broad and small intensity of the meridional reflection ("m" in Figure 7E,E″), it is not possible to establish whether the daughter lamellae are in the α form (Figures 3B,C and 4B), in the γ form (Figures 3D and 4C), and/or in α/γ disordered modifications (Figure 3E). This is a rare example[13] of a crosshatched texture that develops during stretching at room temperature. Generally, crosshatches develop by stretching commercial iPP samples at temperatures higher than 80−90 °C.[8a,36−39]

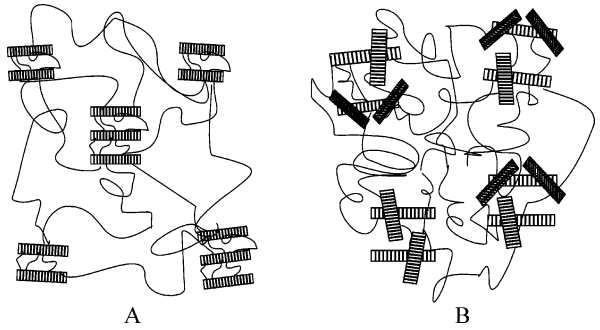

Figure 9. Schematic diagrams illustrating elastomeric networks where crystallites of iPP act as physical cross-links, (A) network with a more conventional texture and (B) network with a crosshatched texture. The chains belonging to the amorphous phase emerge at the boundary of crystalline lamellae fringed-micelle-like along two opposite directions in (A) and along four nearly perpendicular directions in (B), forming an entangled network.

The X-ray diffraction pattern of the stress-relaxed fiber obtained from the fiber stretched at 700% deformation after removing the tension (fiber W(HS)-700) is reported in Figure 7F,F′. The patterns of Figure 7F,F′ are very similar to those of the stretched fiber (Figure 7E,E′) and are characterized by the presence of three strong equatorial reflections at $2\theta \approx 14$, 17, and 18.6° and a strong diffraction peak at $2\theta \approx 21°$ on the first layer line, indicating that the sample is essentially crystallized in the α form in the standard fiber morphology. Moreover, for the relaxed fiber, the reflection at $2\theta \approx 14°$ appears not only polarized on the equator but also in positions close to the meridian (indicated with "m" in Figure 7F,F″), indicating the presence of crosshatches. It is evident that the structural and morphological transformations induced by stretching at high deformations are irreversible. The fact that the sample recovers almost completely the initial dimensions upon the release of the tension[10] indicates that the formation of a crosshatched texture creates a very efficient elastomeric network, where crystals of the α form or in α/γ disordered modifications act as physical knots. Schematic diagrams that illustrate elastomeric networks of iPP based on a crosshatched texture and a more conventional morphology are shown in Figure 9. Crystals of iPP in conventional morphology (Figure 9A) and in crosshatched texture (Figure 9B) act as knots of the network. The chains belonging to the amorphous phase emerge at the boundary of crystalline lamellae fringed-micelle-like along two opposite directions in the conventional network of Figure 9A and along four nearly perpendicular directions in the network based on a crosshatched texture of Figure 9B, forming an entangled network. Upon stretching, the amorphous chains are oriented along the stretching direction storing the entropic recovery force. The elastomeric network with a crosshatched structure shown in Figure 9B is probably more efficient than that shown in Figure 9A.

Oriented Fibers: Sample W(ES). Unoriented films of the fraction soluble in diethyl ether W(ES) obtained by compression molding are amorphous (Figure 5c), but able to crystallize by stretching.[9−11,23,24] The formation of crystals occurs despite the low degree of stereoregularity and has been attributed to the fact that the fraction W(ES) is characterized by chains with a stereoblock structure where atactic sequences alternate with more stereoregular isotactic sequences and the lengths of isotactic sequences are sufficiently long to allow crystallization.[20]

The X-ray fiber diffraction patterns and the corresponding profiles read along the equatorial line of fibers of the sample

W(ES) obtained by stretching compression-molded films at values of strain ϵ of 100, 500, and 1000% and after releasing the tension are reported in Figure 10.

The ability of the W(ES) fraction to crystallize is already apparent at low deformations ($\epsilon = 100\%$), even though the degree of crystallinity achieved by stretching is very low (<5%). The X-ray fiber diffraction pattern of the film stretched at 100% deformation (Figure 10A), indeed, presents a single sharp reflection on the meridian at $\zeta \approx 0.19$ Å^{-1}. As discussed in the previous section, diffraction patterns of the kind shown in Figure 10A correspond to the case of crystals of the α or γ forms or in disordered modification intermediate between the α and γ forms oriented with the b_α-axis of the α form or the c_γ-axis of the γ form, parallel to the stretching direction and with the chain axes perpendicular to the stretching direction (cross-β, or perpendicular chain axis orientation, Figures 3F and 4D). Accurate measurements of the position of this reflection have been performed by mounting the sample in the tilted fiber geometry and then recording the X-ray fiber diffraction pattern in the oscillation mode (±12°) so that the meridian reflection of Figure 10A appears on the equator. The equatorial profile of the fiber stretched at 100% deformation in the tilted fiber geometry is shown in Figure 10A′. The profile of Figure 10A′ unequivocally indicates that the meridional reflection occurs at $2\theta \approx 17°$, and corresponds to the $(040)_\alpha$ reflection of the α form or $(008)_\gamma$ reflection of the γ form. Because the crystallizable isotactic sequences are very short in the fraction W(ES), and short isotactic sequences crystallize in the γ form more easily than in the α form,[14,15,19,20] the fiber stretched at $\epsilon = 100\%$ is probably characterized by crystals in the γ form or in α/γ disordered modifications very close to the γ form in the cross-β orientation.

The diffraction pattern of the stress-relaxed fiber W(ES)-100, obtained by releasing the tension from 100% deformation, (Figure 10B,B′) presents a typical amorphous halo, indicating that crystals in the cross-β orientation, which form by stretching, melt upon releasing the tension.

The azimuthal profile of the reflection at $2\theta \approx 17°$ of the fiber stretched at 100% deformation and of the stress-relaxed fiber W(ES)-100 are compared in Figure 11. It is apparent that the maximum at $\chi \approx \pm 90°$, corresponding to the meridional reflection in the stretched fiber (Figure 11A, curve a), almost disappears in the stress-relaxed fiber and the intensity distribution along χ becomes rather uniform upon releasing the tension (Figure 11B, curve a), confirming the melting of the crystals. The stress-induced crystallization of the fraction W(ES) with crystals in the cross-β orientation, followed by the melting of the crystals upon releasing the tension is reversible. Stretching the amorphous sample at the low value of strain of 100% induces formation of crystals in disordered modifications close to the γ form in the perpendicular chain axis orientation (cross-β); the crystals melt upon releasing the tension. At these low deformations, the fraction W(ES) behaves as a weak gum elastomer and presents a low residual deformation upon releasing the tension.[10]

The unique crystallization mode of the fraction W(ES) at low and moderate deformations may be due to the intrinsic structural features of the γ form. Indeed, the nonparallel arrangement of chain axes in the crystals, typical of the γ form, and the easy inclusion of defects in this polymorph of iPP,[13,14,19] makes the crystallization of the short isotactic sequences of this fraction easier.[20] The crystals that form by stretching should be rather short in the directions parallel to the chain axes, and longer along the c_γ-axis (b_α-axis) direction (Figure 1), so that the

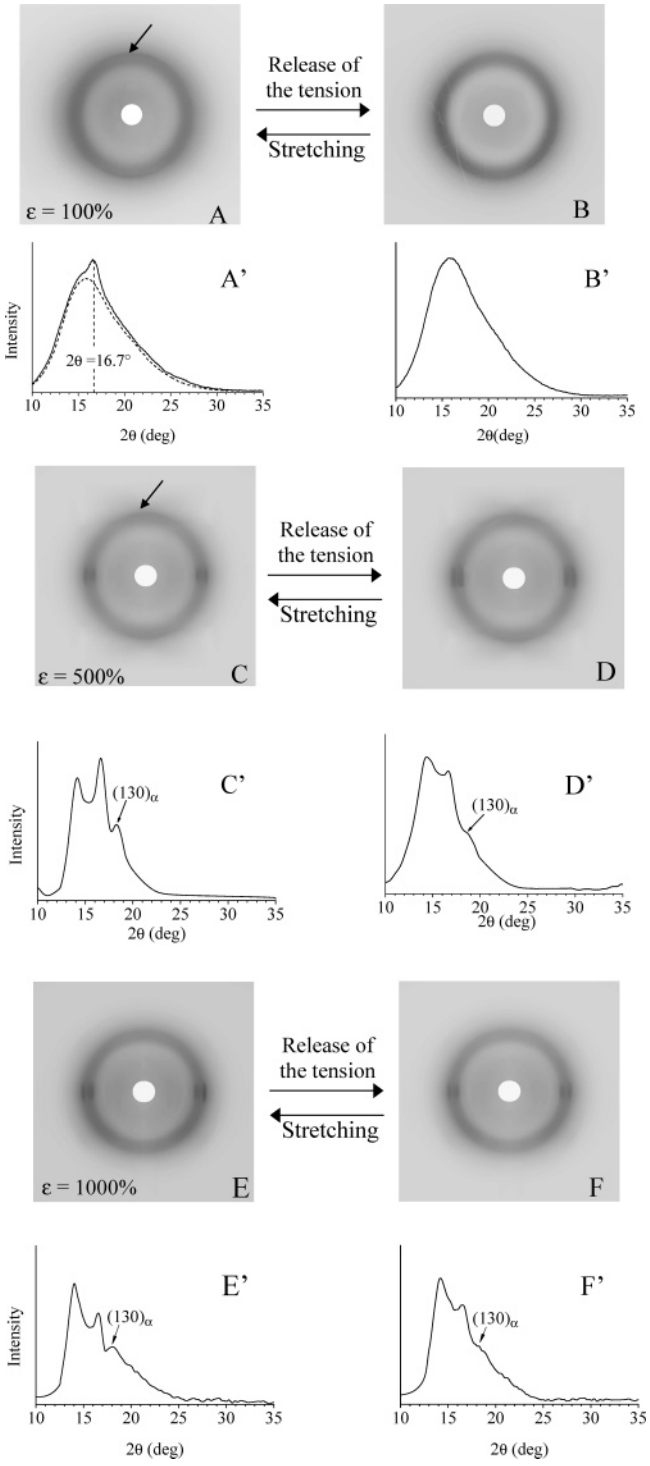

Figure 10. X-ray fiber diffraction patterns (A−F) and corresponding profiles read along the equatorial lines (B′−F′), of fibers of the sample W(ES), obtained by stretching compression molded films at the indicated elongation, keeping the fiber in tension (A, C, E) and after removing the tension (B, D, F). The profiles (C′−F′) have been subtracted for the background intensity and the contribution of the amorphous phase. The $(130)_\alpha$ reflection at $2\theta = 18.6°$ typical of the α form of iPP is indicated. The diffraction profile reported in A′ corresponds to the equatorial X-ray diffraction profile of a fiber of the sample W(ES) obtained by stretching at 100% deformation, recorded by mounting the sample with the fiber axis normal to the axis of the cylindrical camera and normal to the X-ray incident beam (tilted fiber geometry) so that the meridional reflection at $2\theta \approx 17°$ ($(040)_\alpha$ reflection of the α form and $(008)_\gamma$ reflection of the γ form) indicated with an arrow in A, appears on the equator (A′). In A′, the amorphous contribution (dashed line) is also indicated.

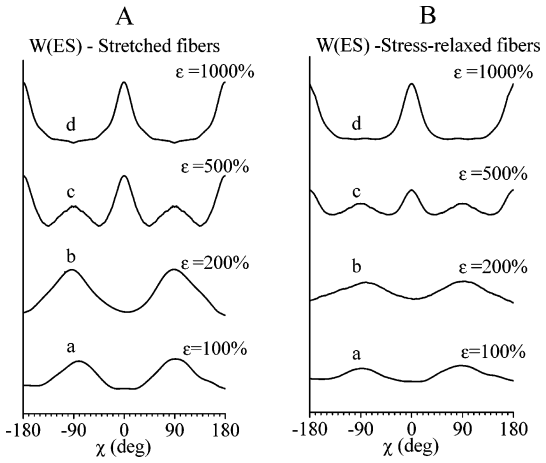

Figure 11. X-ray diffraction azimuthal profiles of the reflection at $2\theta = 17°$ in the X-ray fiber diffraction patterns of sample W(ES) stretched at the indicated values of deformation (Figure 10). The azimuthal scans are reported for fibers obtained by stretching compression molded films at the indicated elongation, keeping the fiber under tension (A) and after removing the tension (B).

resulting elongated entities assume the cross-β orientation, with the longest axis directed more easily parallel to the fiber axis.[14] The dimension of these crystals in the direction parallel to the chain axes is lower than a critical value and, therefore, the crystals melt by releasing the tension.

At higher values of strain, the elongated crystals that form in the W(ES) fraction experience the tensile stress field more efficiently. At 500% deformation, the reflection at $2\theta \approx 17°$ appears polarized both on the equator and on the meridian (Figure 10C,C′). Furthermore, also weak $(110)_\alpha$ and $(130)_\alpha$ reflections of the α form at $2\theta \approx 14$ and 18.6°, respectively, appear on the equator (Figure 10C′). This indicates that both crystals of disordered modifications more similar to the γ form and of disordered modifications closer to the α form are obtained with increasing deformation. Because in the crystals close to the α form, the fraction of consecutive bilayers with parallel chains is prevalent over that of crystals with perpendicular chains, these crystals assume more easily the parallel chain axis orientation, whereas the crystals that assume the cross-β orientation are probably those characterized by structural features closer to the γ form. It is worth noting that, in the X-ray fiber diffraction pattern of the fiber stretched at $\epsilon = 500\%$, the reflections on the first layer line due to the helical periodicity of the chains are apparently absent because of too low intensity. This may be due to the fact that, because the lengths of crystallizable sequences are very short, the degree of crystallinity achieved by stretching is very low and the size of the crystals in the direction parallel to chain axes is also very small.

Crystals formed by stretching at 500% deformation partially melt after removing the tension. The X-ray diffraction pattern along the equator of the fiber W(ES)-500 (Figure 10D,D′) exhibits only two weak equatorial reflections at $2\theta = 14$ and 17° with a shoulder at $2\theta = 18.6°$. The reflection at $2\theta = 17°$ shows only a weak polarization on the equator (Figures 10D and curve c of Figure 11B). This indicates that crystals in the cross-β orientation melt after removing the tension. Crystals that develop by stretching in the parallel chain axis orientation instead are more stable than those in the cross-β orientation. Furthermore, the degree of orientation achieved by stretching at 500% deformation is partially lost upon the release of the tension, as indicated by the fact that the distribution of intensity along the azimuthal arc of the reflection at $2\theta = 17°$ is more uniform than in the stretched fiber (Figure 11B, curve c).

The melting−recrystallization process of crystals in the α/γ disordered modifications in the cross-β orientation is reversible also at 500% deformation; correspondingly, the sample W(ES) shows elastic behavior with very low residual deformations after relaxation from 500% deformation.[10]

Finally, the sample W(ES) stretched at 1000% deformation shows X-ray fiber diffraction patterns (Figure 10E,E′, and curve d of Figure 11A) with two weak maxima at $2\theta = 14$ and 17°, exclusively polarized on the equator, corresponding to the $(110)_\alpha$ and $(040)_\alpha$ reflections, and a broad $(130)_\alpha$ reflection at $2\theta = 18.6°$ of the α form (Figure 10E′). This indicates that the fiber is characterized by crystals in α/γ disordered modifications, close to the α form, oriented with chain axes parallel to the stretching direction, as in a standard fiber morphology. The apparent absence of the reflections on the first layer line typical of the α and γ forms is due to the low degree of crystallinity and to the very short length of crystallizable sequences, consistent with the low degree of stereoregularity of the fraction W(ES). Crystals that form at 1000% deformation indeed include a large amount of structural disorder and exhibit very low dimensions, especially along the direction parallel to the chain axes.

The diffraction patterns of the stress-relaxed fiber W(ES)-1000 (Figure 10F,F′ and curve d of Figure 11B) are quite similar to those of the stretched fiber (Figure 10E,E′, and curve d of Figure 11A), even though the equatorial reflections at $2\theta \approx 14$, 17, and 18.6° are less intense than those of the stretched fiber. This indicates that crystals that develop by stretching partially melt upon releasing the tension. However, also at 1000% deformation, the sample presents an elastomeric behavior, although the permanent deformation upon the release of the tension is higher than that at 500% deformation.[10] The weak elastomeric network is ensured by both the presence of the small fraction of crystals and by entanglement of the chains in the amorphous phase. However, because the crystallinity remains very low (<5%), the fraction W(ES) presents elastomeric properties more similar to those of high-molecular-weight atactic polypropylene[14] than to those of the more stereoregular fraction W(HS).

Conclusions

The structural transformations and textures, which may develop during stretching of metallocene-made iPP samples, are often complicated by the simultaneous presence of the γ and α forms, and the tendency of the α form to nucleate by epitaxy lamellar branching, forming a crosshatched network. The similarities of the diffraction patterns of the α and γ forms and the presence of structural disorder in the crystals do not allow an easy interpretation of the diffraction data. We have illustrated a method of analysis of the structural and textural transformations that may occur during stretching based on the calculation of schematic X-ray fiber diffraction patterns of model structures, where the crystals assume limit mode of orientations, and the comparison of the calculated and experimental diffraction patterns recorded during stretching. The samples used to illustrate this method have been chosen in the large variety of the nowadays available iPP microstructures, with the aim of providing representative examples of possible morphologies and structural transformations that may occur in uniaxially drawn samples.

It is shown that a large number of phenomena are involved during stretching: (i) the transformation of the γ form into the α form through the formation of a continuum of disordered modifications intermediate between the α and γ forms; (ii) the

development, at low deformations, of crystals of the γ form in the "cross-β" orientation, i.e., with chain axes oriented perpendicular or nearly perpendicular to the stretching directions; (iii) the development, at high deformations, of a crosshatched structure, due to epitaxial growth of daughter lamellae with chain axes perpendicular to the stretching directions, on crystals of the α form oriented with chain axes parallel to the fiber axes (mother lamellae).

The nonstandard mode of orientation of γ crystals with chain axes perpendicular to a fiber axis (perpendicular chain axis orientation or cross-β) mainly involves crystals of the γ form frozen in strained regions of the polymer matrix. Its development may be ascribed to the peculiar architecture of the γ form, consisting in a nearly perpendicular arrangement of chain axes in the unit cell and to the elongated shape of the lamellae of the γ form in the direction normal rather than parallel to the chain axes. At low draw ratios, the chain axes, which emerge at the crystal boundaries according to two mutually perpendicular directions, act as anchors for the γ crystals in the perpendicular chain axis orientation. At high draw ratios, these crystals are forced to assume the orientation with chain axes parallel to the stretching direction, as in the standard fiber morphology, and transform into the α form.

The development of these peculiar textures during stretching in elastomeric iPP samples, having a stereoblock microstructure, results in elastic properties in a large deformation range due to the fact that these textural changes are reversible. The stress-induced crystallization of the γ form or of α/γ disordered modifications close to the γ form, the development of cross-β orientation, followed by melting and/or flip−flop reorientation of lamellae with no preferred orientation by releasing the tension, are reversible processes that ensure elastic properties of these materials in a large range of deformations.

Acknowledgment. Financial support from the "Ministero dell'Istruzione, dell'Università e della Ricerca" (PRIN 2004) is gratefully acknowledged. This paper is dedicated to our teacher Prof. Paolo Corradini.

References and Notes

(1) Mejer, H. E. H., Ed.; *Processing of Polymers*; VCH: New York, 1997; Vol. 18.
(2) Liedauer, S.; Eder, G.; Janeschitz-Kriegl, H.; Jorschow, P.; Geymayer, W.; Ingolic, E. *Int. Polym. Process.* **1993**, *8*, 236.
(3) Tribout, C.; Monasse, B.; Haudin, J. M. *Colloid Polym. Sci.* **1996**, *274*, 197.
(4) Kumaraswamy, G.; Issaian, A. M.; Kornfield, J. A. *Macromolecules* **1999**, *32*, 7537.
(5) Elmoumni, A.; Winter H. H.; Waddon, A. J.; Fruitwala, H. *Macromolecules* **2003**, *36*, 6453.
(6) Schimanski, T.; Peijs, T.; Lemstra, P. J.; Loos, J. *Macromolecules* **2004**, *37*, 1818.
(7) Kalay, G.; Bevis, M. J. *J. Polym. Sci., Part B: Polym. Phys*. **1997**, *35*, 241, 265.
(8) (a) Somani, R. H.; Hsiao, B. S.; Nogales, A.; Srinivas, S.; Tsou, A. H.; Sics, I.; Balta-Calleja, F. J.; Ezquerra, T. A. *Macromolecules* **2000**, *33*, 9385. (b) Chu, B.; Hsiao, B. S. *Chem. Rev*. **2001**, *101*, 1727; Ran, S.; Zong, X.; Fang, D.; Hsiao, B. S.; Chu, B.; Cunniff, P. M.; Phillips, R. A. *J. Mater. Sci.* **2001**, *36*, 3071; Somani, R. H.; Hsiao, B. S.; Nogales, A.; Fruitwala, H.; Srinivas, S.; Tsou, A. H. *Macromolecules* **2001**, *34*, 5902; Wang, Z.-G.; Hsiao, B. S.; Srinivas, S.; Brown, G. M.; Tsou, A. H.; Cheng, S. Z. D.; Stein, R. S. *Polymer* **2001**, *42*, 7561; Nogales, A.; Hsiao, B. S.; Somani, R. H.; Srinivas, S.; Tsou, A. H.; Balta-Calleja, F. J.; Ezquerra, T. A. *Polymer* **2001**, *42*, 5247; Ran, S.; Zong, X.; Fang, D.; Hsiao, B. S.; Chu, B.; Phillips, R. A. *Macromolecules* **2001**, *34*, 2569.
(9) Wiyatno, W.; Pople, J. A.; Gast. A. P.; Waymouth, R. M.; Fuller, G. G. *Macromolecules* **2002**, *35*, 8488, 8498.
(10) Wiyatno, W.; Fuller, G. G.; Pople, J. A.; Gast. A. P.; Chen, Z.-R.; Waymouth, R. M.; Myers, C. L. *Macromolecules* **2003**, *36*, 1178.
(11) Wiyatno, W.; Chen, Z.-R.; Liu, X.; Waymouth, R. M.; Krukonis, V.; Brennan, K. *Macromolecules* **2004**, *37*, 701.
(12) Choi, D.; White, J. L. *Polym. Eng. Sci.* **2004**, *44*, 210.
(13) Auriemma, F.; De Rosa, C.; Boscato, T.; Corradini, P. *Macromolecules* **2001**, *34*, 4815.
(14) De Rosa, C.; Auriemma, F.; Perretta, C. *Macromolecules* **2004**, *37*, 6843.
(15) De Rosa, C.; Auriemma, F.; Di Capua A.; Resconi, L.; Guidotti, S.; Camurati, I.; Nifant'ev, I. E.; Laishevtsev, I. P. *J. Am. Chem. Soc.* **2004**, *126*, 17040.
(16) De Rosa, C.; Auriemma, F.; De Lucia, G.; Resconi, L. *Polymer* **2005**, *46*, 9461.
(17) Thomann, R.; Wang, C.; Kressler, J.; Müllhaupt, R. *Macromolecules* **1996**, *29*, 8425.
(18) Alamo, R.; Kim, M.-H.; Galante, M. J.; Isasi, D. R.; Mandelkern, L. *Macromolecules*, **1999**, 32, 4050.
(19) Auriemma, F.; De Rosa, C. *Macromolecules* **2002**, *35*, 9057.
(20) De Rosa, C.; Auriemma, F.; Circelli, T.; Waymouth, R. M. *Macromolecules* **2002**, *35*, 3622.
(21) De Rosa, C.; Auriemma, F.; Circelli, T.; Longo, P.; Boccia, A. C. *Macromolecules* **2003**, *36*, 3465.
(22) De Rosa, C.; Auriemma, F.; Spera, C.; Talarico, G.; Tarallo, O. *Macromolecules* **2004**, *37*, 1441.
(23) Coates, G. W.; Waymouth, R. M. *Science* **1995**, *267*, 217.
(24) Schonherr, H.; Wiyatno, W.; Pople, J.; Frank, C. W.; Fuller, G. G.; Gast, A. P.; Waymouth, R. M. *Macromolecules* **2002**, *35*, 2654.
(25) Schönherr, H.; Waymouth, R. M.; Frankk, C. W. *Macromolecules* **2003**, *36*, 2412.
(26) De Rosa, C.; Auriemma, F.; Spera, C.; Talarico, G.; Gahleitner, M. *Polymer* **2004**, *45*, 5875.
(27) Resconi, L.; Cavallo, L.; Fait, A.; Piemontesi, F. *Chem. Rev.* **2000**, *100*, 1253.
(28) Balboni, D.; Moscardi, G.; Baruzzi, G.; Braga, V.; Camurati, I.; Piemontesi, F.; Resconi, L.; Nifant'ev, I. E.; Venditto, V.; Antinucci, S. *Macromol. Chem. Phys.* **2001**, *202*, 1780.
(29) Brückner, S.; Meille, S. V. *Nature* **1989**, *340*, 455.
(30) Natta, G.; Corradini, P. *Nuovo Cimento Suppl.* **1960**, *15*, 40.
(31) Lotz, B.; Graff, S.; Straupè, C.; Wittmann, J. C. *Polymer* **1991**, *32*, 2902.
(32) Wittmann, J. C.; Lotz, B. *Prog. Polym. Sci.* **1990**, *15*, 909.
(33) Dean, D. M.; Rebenfeld, L.; Register, R. A.; Hsiao, B. S. *J. Mater. Sci.* **1998**, *33*, 4797.
(34) Dean, D. M.; Register, R. A. *J. Polym. Sci., Part B: Polym. Phys.* **1998**, *36*, 2821.
(35) Resconi, L.; Piemontesi, F.; Camurati, I.; Sudmeijer, O.; Ninfant'ev, I. E.; Ivchenko, K. V.; Kuz'mina, L. *J. Am. Chem. Soc.* **1998**, *120*, 2308.
(36) Nadella, H. P.; Henson, H. M.; Spruiell, J. E.; White, J. L. *J. Appl. Polym. Sci.* **1977**, *21*, 3003.
(37) Fung, P. Y. F.; Orlando, E.; Carr, S. H. *Polym. Eng. Sci.* **1973**, *13*, 295.
(38) Anderson, P. G.; Carr, S. H. *J. Mater. Sci.* **1975**, *10*, 870.
(39) Lu, F. M.; Spruiell, J. E. *J. Appl. Polym. Sci.* **1987**, *34*, 1521.
(40) Lotz, B.; Wittmann, J. C. *J. Polym. Sci., Part B: Polym. Phys.* **1986**, *24*, 1541.
(41) Choi, D.; White, J. L. *Int. Polym. Process.* **1998**, *13*, 78.
(42) Choi, D.; White, J. L. *Int. Polym. Process.* **2000**, *15*, 398.
(43) Awaya, H. *Polym. Lett.* **1966**, *4*, 1267.
(44) Gedder, A. J.; Parker, K. T.; Atkins, E. D. T.; Beighton, E. *J. Mol. Biol.* **1968**, *32*, 343.
(45) Stocker, W.; Maganov, S. N.; Cantow, H.-J.; Wittmann, J. C.; Lotz, B. *Macromolecules* **1993**, *26*, 5915.
(46) R. Hiss, S. Hobeika, C. Lynn and G. Strobl *Macromolecules* **1999**, *32*, 4390; Y. Men and G. Strobl *J. Macromol. Sci., Phys.* **2001**, *B40*, 775.

MA0609127